

Beyond-mean-field approach to low-lying spectra of Λ hypernuclei

Kouichi HAGINO^{1,2}, Hua MEI^{1,3}, Jiangming YAO^{1,3,4}, and Toshio MOTOMA^{5,6}

¹*Department of Physics, Tohoku University, Sendai 980-8578, Japan*

²*Research Center for Electron Photon Science, Tohoku University, 1-2-1 Mikamine, Sendai 982-0826, Japan*

³*School of Physical Science and Technology, Southwest University, Chongqing 400715, China*

⁴*Department of Physics and Astronomy, University of North Carolina, Chapel Hill, North Carolina 27516-3255, USA*

⁵*Laboratory of Physics, Osaka Electro-Communication University, Neyagawa 572-8530, Japan*

⁶*Yukawa Institute for Theoretical Physics, Kyoto University, Kyoto 606-8502, Japan*

(Received)

Taking the hypernucleus ${}^{13}_{\Lambda}\text{C}$ as an example, we illustrate the microscopic particle-rotor model for low-lying spectra of hypernuclei. This approach is based on the beyond-mean-field method, with the particle number and angular momentum projections. The quantum fluctuation of the mean-field is also taken into account for the core nucleus using the generator coordinate method. We show that the impurity effect of Λ hyperon, such as a change in $B(E2)$, is well described with this model. Our calculation indicates that the most important impurity effect in sd -shell hypernuclei is a change in a deformation parameter rather than in a nuclear size.

KEYWORDS: hypernuclei, low-lying spectrum, impurity effect, beyond-mean-field approach

1. Introduction

The development in Λ -hypernuclear spectroscopy has enabled one to explore several aspects of hypernuclear structure [1]. The measured energy spectra and electric multipole transition strengths in low-lying states have in fact provided rich information on the Λ -nucleon interaction in nuclear medium as well as on the impurity effect of Λ particle. Many theoretical methods have been developed to investigate the spectroscopy of hypernuclei, such as the cluster model [2, 3], the shell model [4], the ab-initio method [5], the antisymmetrized molecular dynamics (AMD) [6], and self-consistent mean-field models [7–10]. Among them, the self-consistent mean-field approach is the only method which can be globally applied from light to heavy hypernuclei.

Even though the self-consistent mean-field approach provides an intuitive view of nuclear deformation, it is a drawback of this method that it does not yield a spectrum in the laboratory frame, since the approach itself is formulated in the body-fixed frame. This can actually be overcome by going beyond the mean-field approximation, in particular, by carrying out the angular momentum projection. One can also take into account the quantum fluctuation of the mean-field wave function by superposing many Slater determinants with the generator coordinate method (GCM). When the pairing correlation is important, the particle number projection can also be implemented. Such scheme has been referred to as a beyond-mean-field approach, and has rapidly been developed in the nuclear structure physics for the past decade [11, 12].

In this contribution, we present a new method for low-lying states of hypernuclei based on the beyond-mean-field approach [13, 14]. In this method, we first apply the beyond-mean-field approach to a core nucleus. Low-lying states of hypernuclei are then constructed by coupling a Λ particle to the

core nucleus states. We thus call this approach the microscopic particle-rotor model, in which the rotor part is described with the microscopic beyond-mean-field method. See Refs. [15–18] for other different types of application of the beyond-mean-field approach to hypernuclei, which are complementary to the present microscopic particle-rotor model. We shall apply the microscopic particle-rotor model to the ${}^{13}_{\Lambda}\text{C}$ hypernucleus and discuss the impurity effect in this hypernucleus.

2. Microscopic particle-rotor model

We consider a hypernucleus, which consists of a Λ particle and an even-even core nucleus. In the microscopic particle-rotor model, the wave function for the whole Λ hypernucleus with the angular momentum J and its z -component M is given as

$$\Psi_{JM}(\mathbf{r}, \{\mathbf{r}_N\}) = \sum_{n,j,\ell,l} R_{j\ell nl}(r) [\mathcal{Y}_{j\ell}(\hat{\mathbf{r}}) \otimes \Phi_{nl}(\{\mathbf{r}_N\})]^{(JM)}, \quad (1)$$

where \mathbf{r} and \mathbf{r}_N are the coordinates of the Λ hyperon and the nucleons, respectively. In this equation, $\mathcal{Y}_{j\ell}(\hat{\mathbf{r}})$ is the spin-angular wave function for the Λ hyperon, while $|\Phi_{nl}\rangle$ is the wave functions for the low-lying states of the nuclear core. The latter is constructed from the mean-field wave functions as,

$$|\Phi_{nIM_I}\rangle = \int d\beta f_{nI}(\beta) \hat{P}_{M_I K}^I \hat{P}^N \hat{P}^Z |\varphi(\beta)\rangle, \quad (2)$$

where β is the quadrupole deformation parameter and $|\varphi(\beta)\rangle$ is the mean-field wave function at β obtained with the constrained mean-field approximation. Here we have assumed that the core nucleus has axial symmetric shape. $\hat{P}_{M_I K}^I$, \hat{P}^N , and \hat{P}^Z are the projections operators for the angular momentum, the neutron number, and the proton number, respectively. The weight function $f_{nI}(\beta)$ in Eq. (2) is determined by the variational principle, that is, by solving the Hill-Wheeler equation.

We assume that the total Hamiltonian for this system is given by,

$$\hat{H} = \hat{T}_{\Lambda} + \sum_{i=1}^{A_c} v_{N\Lambda}(\mathbf{r}, \mathbf{r}_{N_i}) + \hat{H}_c, \quad (3)$$

where A_c is the mass number of the core nucleus. Here, the first term is the kinetic energy of Λ hyperon and the second term denotes a nucleon-hyperon interaction. The last term, \hat{H}_c , is the Hamiltonian for the core nucleus, which is solved with the beyond-mean-field approach. With the Hamiltonian, Eq. (3), one can derive the coupled-channels equations for the radial wave functions, $R_{j\ell nl}(r)$, in which the coupling potentials are given in terms of the transition densities [13, 14]. The solutions of the coupled-channels equations provide the spectrum of the hypernucleus as well as the transition probabilities among the low-lying states.

3. Application to the ${}^{13}_{\Lambda}\text{C}$ hypernucleus

We now apply the microscopic particle-rotor model to the ${}^{13}_{\Lambda}\text{C}$ hypernucleus, even though the model can be applied also to even heavier hypernuclei, such as ${}^{155}_{\Lambda}\text{Sm}$. To this end, we use the relativistic point coupling model with the PC-F1 parameter set [19] for the effective nucleon-nucleon interaction. For the nucleon-hyperon interaction, we use a simple relativistic zero-range interaction with a repulsive vector-type and an attractive scalar-type terms [13, 14],

$$v_{N\Lambda}(\mathbf{r}, \mathbf{r}_N) = \alpha_V^{N\Lambda} \delta(\mathbf{r} - \mathbf{r}_N) + \alpha_S^{N\Lambda} \gamma_{\Lambda}^0 \delta(\mathbf{r} - \mathbf{r}_N) \gamma_N^0, \quad (4)$$

where γ^0 is a Dirac matrix. The parameters $\alpha_V^{N\Lambda}$ and $\alpha_S^{N\Lambda}$ are determined so as to reproduce the empirical Λ binding energy of ${}^{13}_{\Lambda}\text{C}$. The coupled-channels equations for the radial wave functions,

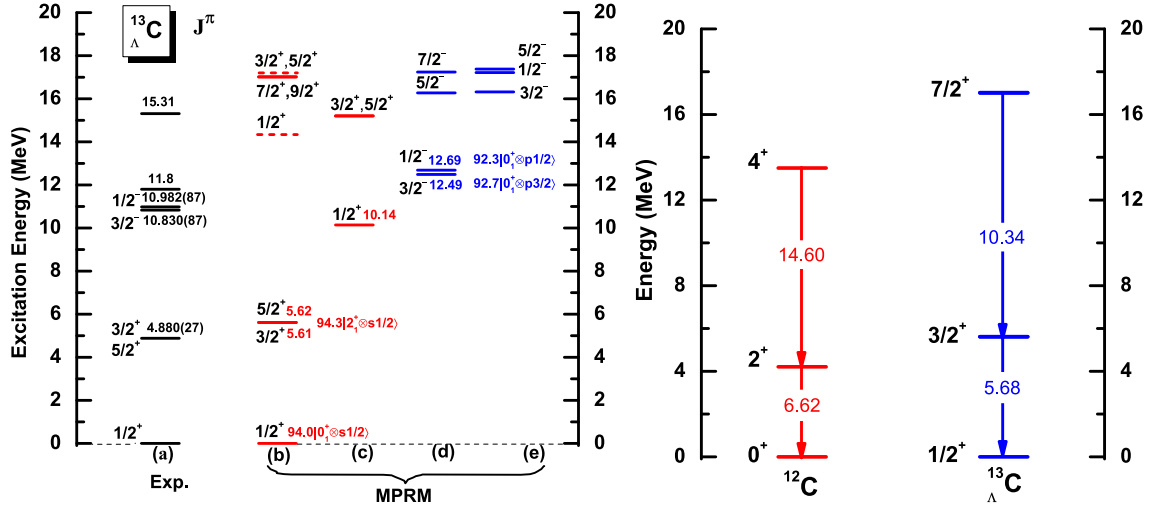


Fig. 1. The left panel: the spectrum of the $^{13}_{\Lambda}\text{C}$ hypernucleus obtained with the microscopic particle-rotor model. The experimental data are taken from Ref. [1]. The right panel: a comparison of calculated $E2$ transition strengths, $B(E2)$, for ^{12}C and $^{13}_{\Lambda}\text{C}$, given in units of $e^2 \text{fm}^4$.

$R_{j\ell n l}(r)$, are solved by expanding $R_{j\ell n l}(r)$ on a spherical harmonic oscillator basis with 18 major shells. To this end, we include the 0_1^+ , 2_1^+ , 4_1^+ , 0_2^+ , 2_2^+ , and 4_2^+ states in the core nucleus, ^{12}C .

The left panel of Fig. 1 shows the low-lying spectrum of $^{13}_{\Lambda}\text{C}$ so obtained. One can see that the low-lying spectrum for $^{13}_{\Lambda}\text{C}$ is well reproduced, although the excitation energies are slightly overestimated. This calculation indicates the ground state rotational band of $^{13}_{\Lambda}\text{C}$ shown in the column (b), that is, the ground state $1/2^+$ and the two doublets of $(5/2^+, 3/2^+)$ and $(9/2^+, 7/2^+)$, mainly consist of the configuration of $\Lambda s_{1/2}$ coupled to the ground rotational band (that is, 0_1^+ , 2_1^+ , and 4_1^+) of the core nucleus, ^{12}C . The doublet states are almost degenerate in energy, the energy difference being only 10 keV for each of the two doublets. The levels in the column (c) correspond to the configuration of $\Lambda s_{1/2}$ coupled to the second rotational band ($n = 2$) in ^{12}C . These states share similar features as those in the ground state band shown in the column (b).

In the negative-parity states shown in the column (d), the dominant configuration in the wave functions is that with the Λ particle in the p orbitals coupled to the ground state rotational band of the core nucleus. That is, the first $3/2^-$ and $1/2^-$ states consist mainly of $0_1^+ \otimes \Lambda p_{3/2}$ and $0_1^+ \otimes \Lambda p_{1/2}$, respectively, as is indicated in the figure. The energy splitting between these states is as small as 199 keV, which reflects mainly the spin-orbit splitting of Λ hyperon in the $p_{3/2}$ and $p_{1/2}$ states. The obtained splitting is in a good agreement with the empirical value, $152 \pm 54 \pm 36$ keV [20].

In contrast to the first $1/2^-$ and $3/2^-$ states, the second $1/2^-$ and $3/2^-$ states in the column (e) show a large configuration mixing. That is, the fraction of the $0_1^+ \otimes \Lambda p_{1/2}$ and $2_1^+ \otimes \Lambda p_{3/2}$ configurations in the wave function for the $1/2^-$ state is 0.60 and 0.38, respectively, while the fraction of the $2_1^+ \otimes \Lambda p_{3/2}$ and $2_1^+ \otimes \Lambda p_{1/2}$ configurations is 0.54 and 0.45, respectively, in the wave function for the $3/2^-$ state [14]. This large admixture of the configurations is due to the fact that there are two states whose unperturbed energy in the single-channel calculations is close to one another. A similar admixture occurs in other hypernuclei as well, such as $^9_{\Lambda}\text{Be}$ and $^{21}_{\Lambda}\text{Ne}$ [13, 14], which however show this feature already in the first $1/2^-$ and $3/2^-$ states. The difference between $^{13}_{\Lambda}\text{C}$ and a pair of ($^9_{\Lambda}\text{Be}$, $^{21}_{\Lambda}\text{Ne}$) originates mainly from the sign of the quadrupole deformation of the core nucleus, that is, an oblate deformation for ^{12}C and a prolate deformation for ^8Be and ^{20}Ne [14].

The right panel of Fig. 1 shows a comparison of the calculated $E2$ transition strengths for low-lying positive parity states of $^{13}_{\Lambda}\text{C}$ with those of the core nucleus, ^{12}C . In general, these transition

strengths cannot be compared directly due to different angular momentum factors. However, for the transition from the $3/2^+$ and the $5/2^+$ states to the $1/2^+$ state, such factor becomes trivial, and the transition strength can be directly interpreted as the that for the core nucleus from the 2^+ to the 0^+ states [14]. Our calculation indicates that the $E2$ transition strength for $2_1^+ \rightarrow 0_1^+$ in ^{12}C is significantly reduced, by a factor of $\sim 14\%$, due to the addition of a Λ particle. The main cause of the reduction in the $B(E2)$ value is the reduction in nuclear deformation. According to our calculation, the proton radius r_p is reduced from 2.44 fm to 2.39 fm by adding a Λ particle to the ^{12}C nucleus, which leads to about 7.9% reduction in r_p^4 . In contrast, the deformation parameter β is altered from -0.29 to -0.23 , leading to 37.1% reduction in β^2 . This clearly indicates that the change in deformation is the most important impurity effect in sd -shell hypernuclei. A similar conclusion has been reached also in Ref. [18].

4. Summary

We have presented the microscopic particle-rotor model for the low-lying states of single- Λ hypernuclei. In this formalism, the wave functions for hypernuclei are constructed by coupling the Λ hyperon to the low-lying states of the core nucleus. Applying this method to $^{13}_{\Lambda}\text{C}$, we have well reproduced the experimental energy spectrum of this hypernucleus. We have also found that the deformation is reduced by adding a Λ particle in the positive-parity states, leading to a reduction in the $B(E2)$ value from the first 2^+ to the ground states in the core nucleus.

In this paper, for simplicity, we have assumed the axial deformation for the core nucleus. An obvious extension of our method is to take into account the triaxial deformation of the core nucleus. One interesting application for this is $^{25}_{\Lambda}\text{Mg}$, for which the triaxial degree of freedom has been shown to be important in the core nucleus ^{24}Mg .

Acknowledgment

This work was supported by JSPS KAKENHI Grant Number 2640263 and the NSFC under Grant Nos. 11575148 and 11305134.

References

- [1] O. Hashimoto and H. Tamura, Prog. Part. Nucl. Phys. **57**, 564 (2006).
- [2] T. Motoba, H. Bandō, and K. Ikeda, Prog. Theor. Phys. **70**, 189 (1983).
- [3] E. Hiyama, M. Kamimura, K. Miyazaki, and T. Motoba, Phys. Rev. C **59**, 2351 (1999).
- [4] D. J. Millener, Nucl. Phys. **A804**, 84 (2008); **A914**, 109 (2013).
- [5] R. Wirth *et al.*, Phys. Rev. Lett. **113**, 192502 (2014).
- [6] M. Isaka, M. Kimura, A. Doté and A. Ohnishi, Phys. Rev. C **83**, 044323 (2011).
- [7] X. R. Zhou, H.-J. Schulze, H. Sagawa, C. X. Wu, and E.-G. Zhao, Phys. Rev. C **76**, 034312 (2007).
- [8] M. T. Win and K. Hagino, Phys. Rev. C **78**, 054311 (2008).
- [9] Myaing Thi Win, K. Hagino, and T. Koike, Phys. Rev. C **83**, 014301 (2011).
- [10] B.-N. Lu, E.-G. Zhao, and S.-G. Zhou, Phys. Rev. C **84**, 014328 (2011).
- [11] M. Bender, P.-H. Heenen, and P.-G. Reinhard, Rev. Mod. Phys. **57**, 121 (2003).
- [12] J.M. Yao, K. Hagino, Z.P. Li, J. Meng, and P. Ring, Phys. Rev. **C89**, 054306 (2014).
- [13] H. Mei, K. Hagino, J.M. Yao, and T. Motoba, Phys. Rev. **C90**, 064302 (2014).
- [14] H. Mei, K. Hagino, J.M. Yao, and T. Motoba, Phys. Rev. **C91**, 064305 (2015).
- [15] H. Mei, K. Hagino, and J.M. Yao, arXiv:1511.02957 [nucl-th].
- [16] W.X. Xue, J.M. Yao, K. Hagino, Z.P. Li, H. Mei, and Y. Tanimura, Phys. Rev. **C91**, 024327 (2015).
- [17] J.-W. Cui, X.-R. Zhou, and H.-J. Schulze, Phys. Rev. **C91**, 054306 (2015).
- [18] J.M. Yao, Z.P. Li, K. Hagino, M. Thi Win, Y. Zhang, and J. Meng, Nucl. Phys. **A868**, 12 (2011).
- [19] T. Burvenich, D. G. Madland, J. A. Maruhn, and P.-G. Reinhard, Phys. Rev. C **65**, 044308 (2002).
- [20] S. Ajimura *et al.*, Phys. Rev. Lett. **86**, 4255 (2001).